

# Sub-barrier capture reactions with $^{16,18}\text{O}$ and $^{40,48}\text{Ca}$ beams

V.V.Sargsyan<sup>1</sup>, G.G.Adamian<sup>1</sup>, N.V.Antonenko<sup>1</sup>, W. Scheid<sup>2</sup>, and H.Q.Zhang<sup>3</sup>

<sup>1</sup>*Joint Institute for Nuclear Research, 141980 Dubna, Russia*

<sup>2</sup>*Institut für Theoretische Physik der Justus-Liebig-Universität, D-35392 Giessen, Germany*

<sup>3</sup>*China Institute of Atomic Energy, Post Office Box 275, Beijing 102413, China*

(Dated: October 9, 2018)

Various sub-barrier capture reactions with beams  $^{16,18}\text{O}$  and  $^{40,48}\text{Ca}$  are treated within the quantum diffusion approach. The role of neutron transfer in these capture reactions is discussed. The quasielastic and capture barrier distributions are analyzed and compared with the recent experimental data.

## I. INTRODUCTION

From the present experimental data the role of the neutron transfer channel in the capture (fusion) process cannot be unambiguously inferred [1–5]. The fusion excitation functions have been recently measured for the reactions  $^{16}\text{O}+^{76}\text{Ge}$  and  $^{18}\text{O}+^{74}\text{Ge}$  at energies near and below the Coulomb barrier and the fusion barrier distributions have been extracted from the corresponding excitation functions [2]. The fusion enhancement due to the positive  $Q_{2n}$ -value two neutron ( $2n$ ) transfer channel for  $^{18}\text{O}+^{74}\text{Ge}$  has not been revealed as compared with the reference system  $^{16}\text{O}+^{76}\text{Ge}$  [2]. This is very different from the situation for the reactions  $^{40}\text{Ca}+^{124,132}\text{Sn}$  [3] and other systems in literature, which show considerable sub-barrier enhancements. The enhancement appears to be related to the existence of positive  $Q$  values for neutron transfer.

The purpose of this paper is the theoretical explanation of these experimental observations. Within the quantum diffusion approach [4, 5] we try to answer the question how strong the influence of neutron transfer in sub-barrier capture (fusion) reactions  $^{18}\text{O}+^{74}\text{Ge}$ ,  $^{52,50}\text{Cr}$ ,  $^{94,92}\text{Mo}$ ,  $^{112,114,118,120,124,126}\text{Sn}$  and  $^{40,48}\text{Ca}+^{124,132}\text{Sn}$ . This study seems to be important for future experiments indicated in Ref. [2]. In addition, the new structures of the quasielastic and capture barrier distributions at deep sub-barrier energies will be discussed.

## II. MODEL

In the quantum diffusion approach [4, 5] the collisions of nuclei are described with a single relevant collective variable: the relative distance between the colliding nuclei. This approach takes into consideration the fluctuation and dissipation effects in collisions of heavy ions which model the coupling with various channels (for example, coupling of the relative motion with low-lying collective modes such as dynamical quadrupole and octupole modes of the target and projectile [6]). We have to mention that many quantum-mechanical and non-Markovian effects accompanying the passage through the potential barrier are taken into consideration in our formalism [5]. The nuclear deformation effects are taken into account through the dependence of the nucleus-nucleus potential on the deformations and mutual orientations of the colliding nuclei. To calculate the nucleus-nucleus interaction potential  $V(R)$ , we use the procedure presented in Refs. [5]. For the nuclear part of the nucleus-nucleus potential, the double-folding formalism with the Skyrme-type density-dependent effective nucleon-nucleon interaction is used. With this approach many heavy-ion capture reactions at energies above and well below the Coulomb barrier have been successfully described [5]. Note that the diffusion models, which include the quantum statistical effects, were also treated in Refs. [7].

Following the hypothesis of Ref. [8], we assume that the sub-barrier capture in the reactions under consideration mainly depends on the possible two-neutron transfer with the positive  $Q_{2n}$ -value. Our assumption is that, just before the projectile is captured by the target-nucleus (just before the crossing of the Coulomb barrier) which is a slow process, the  $2n$ -transfer ( $Q_{2n} > 0$ ) occurs that can lead to the population of the excited collective states in the recipient nucleus [9]. So, the motion to the  $N/Z$  equilibrium starts in the system before the capture because it is energetically favorable in the dinuclear system in the vicinity of the Coulomb barrier. For the reactions considered, the average change of mass asymmetry is related to the two-neutron transfer. In these reactions the  $2n$ -transfer channel is more favorable than  $1n$ -transfer channel ( $Q_{2n} > Q_{1n}$ ). Since after the  $2n$ -transfer the mass numbers, the deformation parameters of the interacting nuclei, and, correspondingly, the height  $V_b = V(R_b)$  of the Coulomb barrier are changed, one can expect an enhancement or suppression of the capture. This scenario was verified in the description of many reactions [5].

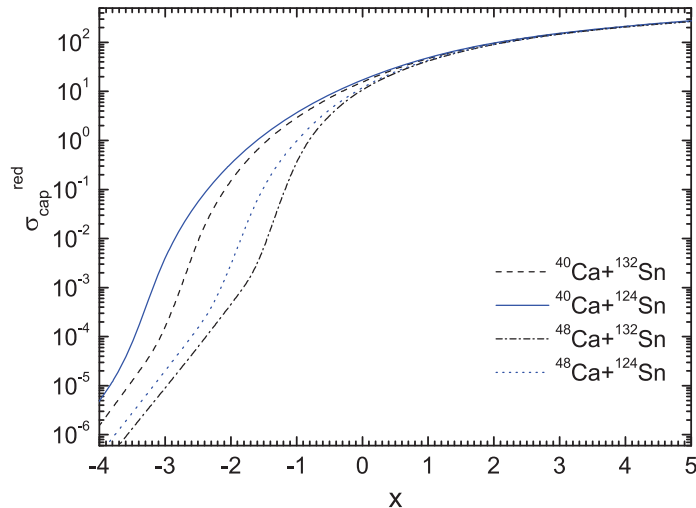


FIG. 1: (Colour online) The calculated reduced capture cross sections versus  $(E_{c.m.} - V_b)/(\hbar\omega_b)$  in the reactions  $^{40}\text{Ca}+^{124}\text{Sn}$  (solid line),  $^{48}\text{Ca}+^{124}\text{Sn}$  (dashed line),  $^{48}\text{Ca}+^{132}\text{Sn}$  (dotted line), and  $^{40}\text{Ca}+^{132}\text{Sn}$  (dash-dotted line).

### III. RESULTS OF CALCULATIONS

All calculated results are obtained with the same set of parameters as in Ref. [5] and are rather insensitive to the reasonable variation of them [5]. Realistic friction coefficient in the momentum  $\hbar\lambda=2$  MeV is used which is close to those calculated within the mean field approaches [10]. The parameters of the nucleus-nucleus interaction potential  $V(R)$  are adjusted to describe the experimental data at energies above the Coulomb barrier corresponding to spherical nuclei. The absolute values of the quadrupole deformation parameters  $\beta_2$  of even-even deformed nuclei are taken from Ref. [11]. In Ref. [11], the quadrupole deformation parameters  $\beta_2$  are given for the first excited  $2^+$  states of nuclei. For the nuclei deformed in the ground state, the  $\beta_2$  in  $2^+$  state is similar to the  $\beta_2$  in the ground state and we use  $\beta_2$  from Ref. [11] in the calculations. For the double magic nucleus  $^{16}\text{O}$ , in the ground state we take  $\beta_2 = 0$ . Since there are uncertainties in the definition of the values of  $\beta_2$  in light- and medium-mass nuclei, one can extract the quadrupole deformation parameters of these nuclei from a comparison of the calculated capture cross sections with the existing experimental data. By describing the reactions  $^{18}\text{O}+^{208}\text{Pb}$ , where there are no neutron transfer channels with positive  $Q$ -values, we extract  $\beta_2 = 0.1$  for the ground-state of  $^{18}\text{O}$  [5]. This extracted value is used in our calculations.

#### A. Effect of neutron transfer in reactions with beams $^{40,48}\text{Ca}$

To eliminate the influence of the nucleus-nucleus potential on the capture (fusion) cross section and to make conclusions about the role of deformation of colliding nuclei and the nucleon transfer between interacting nuclei in the capture (fusion) cross section, a reduction procedure is useful [12]. It consists of the following transformations:

$$E_{c.m.} \rightarrow x = \frac{E_{c.m.} - V_b}{\hbar\omega_b}, \quad \sigma_{cap} \rightarrow \sigma_{cap}^{red} = \frac{2E_{c.m.}}{\hbar\omega_b R_b^2} \sigma_{cap},$$

where  $\sigma_{cap} = \sigma_{cap}(E_{c.m.})$  is the capture cross section at bombarding energy  $E_{c.m.}$ . The frequency  $\omega_b = \sqrt{V''(R_b)/\mu}$  is related with the second derivative  $V''(R_b)$  of the total nucleus-nucleus potential  $V(R)$  (the Coulomb + nuclear parts) at the barrier radius  $R_b$  and the reduced mass parameter  $\mu$ . With these replacements we compared the reduced calculated capture (fusion) cross sections  $\sigma_{cap}^{red}$  for the reactions  $^{40,48}\text{Ca}+^{124,132}\text{Sn}$  (Fig. 1). The choice of the projectile-target combination is crucial, and for the systems studied one can make unambiguous statements regarding the neutron transfer process with a positive  $Q$ -value when the interacting nuclei are double magic or semi-magic spherical nuclei. In this case one can disregard the strong direct nuclear deformation effects. In Fig. 1, one can see that the reduced capture cross sections in the reactions  $^{40}\text{Ca}+^{124,132}\text{Sn}$  with the positive  $Q_{2n}$ -values strongly deviate from those in the reactions  $^{48}\text{Ca}+^{124,132}\text{Sn}$ , where the neutron transfers are suppressed because of the negative  $Q$ -values. After two-neutron transfer in the reactions  $^{40}\text{Ca}(\beta_2 = 0)+^{124}\text{Sn}(\beta_2 = 0.1) \rightarrow ^{42}\text{Ca}(\beta_2 = 0.25)+^{122}\text{Sn}(\beta_2 = 0.1)$  ( $Q_{2n}=5.4$  MeV) and  $^{40}\text{Ca}(\beta_2 = 0)+^{132}\text{Sn}(\beta_2 = 0) \rightarrow ^{42}\text{Ca}(\beta_2 = 0.25)+^{130}\text{Sn}(\beta_2 = 0)$  ( $Q_{2n}=7.3$  MeV) the deformation

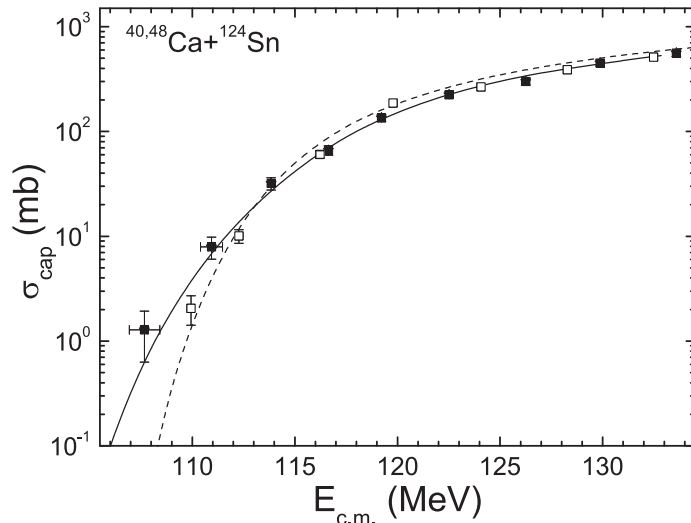


FIG. 2: The calculated capture cross sections versus  $E_{c.m.}$  for the reactions  $^{40}\text{Ca}+^{124}\text{Sn}$  (solid line) and  $^{48}\text{Ca}+^{124}\text{Sn}$  (dashed line). The experimental data for the reactions  $^{40}\text{Ca}+^{124}\text{Sn}$  (solid squares) and  $^{48}\text{Ca}+^{124}\text{Sn}$  (open squares) are from Ref. [3]. In the calculations the barriers were adjusted to the experimental values.

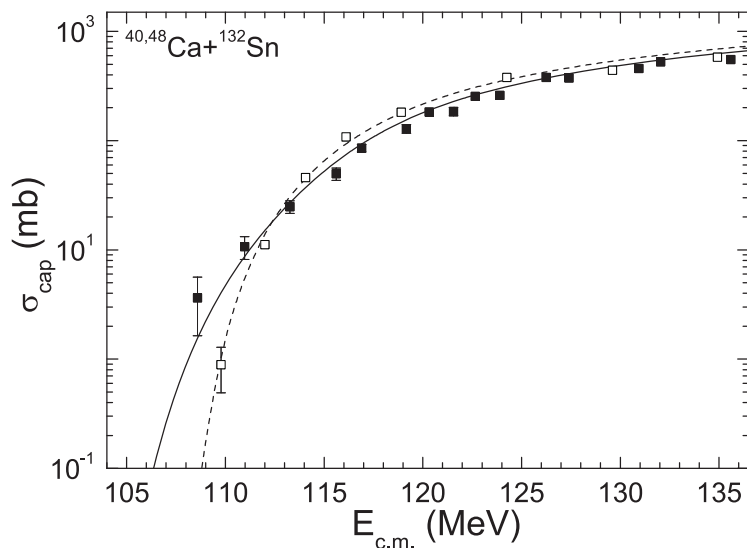


FIG. 3: The calculated capture cross sections versus  $E_{c.m.}$  for the reactions  $^{40}\text{Ca}+^{132}\text{Sn}$  (solid line) and  $^{48}\text{Ca}+^{132}\text{Sn}$  (dashed line). The experimental data for the reactions  $^{40}\text{Ca}+^{132}\text{Sn}$  (solid squares) and  $^{48}\text{Ca}+^{132}\text{Sn}$  (open squares) are from Ref. [3]. In the calculations the barriers were adjusted to the experimental values.

of the light nucleus increases and the mass asymmetry of the system decreases and, thus, the value of the Coulomb barrier decreases and the capture cross section becomes larger (Fig. 1). So, because of the transfer effect the systems  $^{40}\text{Ca}+^{124,132}\text{Sn}$  show large sub-barrier enhancements with respect to the systems  $^{48}\text{Ca}+^{124,132}\text{Sn}$ . We observe that the  $\sigma_{cap}^{red}$  in the  $^{40}\text{Ca}+^{124}\text{Sn}$  ( $^{48}\text{Ca}+^{124}\text{Sn}$ ) reaction are larger than those in the  $^{40}\text{Ca}+^{132}\text{Sn}$  ( $^{48}\text{Ca}+^{132}\text{Sn}$ ) reaction. The reason of that is the nonzero quadrupole deformation of the heavy nucleus  $^{124}\text{Sn}$ . It should be stressed that there are almost no difference between  $\sigma_{cap}^{red}$  in the reactions  $^{40,48}\text{Ca}+^{124,132}\text{Sn}$  at energies above the Coulomb barrier.

In Figs. 2 and 3 one can see a good agreement between the calculated results and the experimental data in the reactions  $^{40,48}\text{Ca}+^{124,132}\text{Sn}$ . This means that the observed capture enhancements in the reactions  $^{40}\text{Ca}+^{124,132}\text{Sn}$  at sub-barrier energies are related to the two-neutron transfer effect. Note that the slope of the excitation function strongly depends on the deformations of the interacting nuclei and, respectively, on the neutron transfer effect.

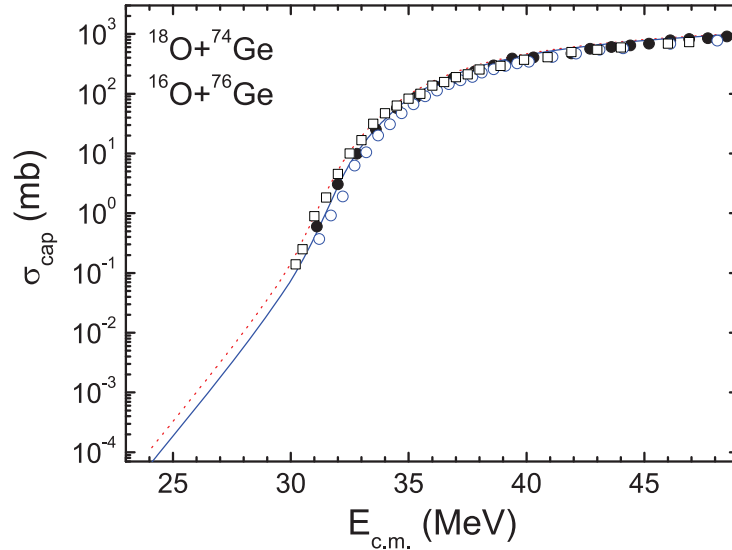


FIG. 4: (Colour online) The calculated (solid line) capture cross sections versus  $E_{c.m.}$  for the reactions  $^{16}\text{O}+^{76}\text{Ge}$  and  $^{18}\text{O}+^{74}\text{Ge}$  (the curves coincide). For the  $^{18}\text{O}+^{74}\text{Ge}$  reaction, the calculated capture cross sections without neutron transfer are shown by dotted line. The experimental data for the reactions  $^{16}\text{O}+^{76}\text{Ge}$  (open circles) and  $^{18}\text{O}+^{74}\text{Ge}$  (open squares) are from Ref. [2]. The experimental data for the  $^{16}\text{O}+^{76}\text{Ge}$  reaction (solid circles) are from Ref. [13].

To describe the reactions  $^{40,48}\text{Ca}+^{132}\text{Sn}$  (Fig. 2) and  $^{48}\text{Ca}+^{124,132}\text{Sn}$  (Fig. 3), we extracted the values of the corresponding Coulomb barrier  $V_b$  for the spherical nuclei. There are differences between the calculated and extracted  $V_b$ . From the direct calculations of the nucleus-nucleus potentials (with the same set of parameters), we obtained  $V_b(^{40}\text{Ca}+^{124}\text{Sn})-V_b(^{48}\text{Ca}+^{124}\text{Sn})=2.3$  MeV,  $V_b(^{40}\text{Ca}+^{132}\text{Sn})-V_b(^{48}\text{Ca}+^{132}\text{Sn})=2.2$  MeV,  $V_b(^{40}\text{Ca}+^{124}\text{Sn})-V_b(^{40}\text{Ca}+^{132}\text{Sn})=1.3$  MeV, and  $V_b(^{48}\text{Ca}+^{124}\text{Sn})-V_b(^{48}\text{Ca}+^{132}\text{Sn})=1.2$  MeV. From the extractions, we got  $V_b(^{40}\text{Ca}+^{124}\text{Sn})-V_b(^{48}\text{Ca}+^{124}\text{Sn})=1.1$  MeV,  $V_b(^{40}\text{Ca}+^{132}\text{Sn})-V_b(^{48}\text{Ca}+^{132}\text{Sn})=1.0$  MeV,  $V_b(^{40}\text{Ca}+^{124}\text{Sn})-V_b(^{40}\text{Ca}+^{132}\text{Sn})=-0.3$  MeV, and  $V_b(^{48}\text{Ca}+^{124}\text{Sn})-V_b(^{48}\text{Ca}+^{132}\text{Sn})=-0.4$  MeV, which seem to be unrealistically small. However, these differences of  $V_b$  do not influence the slopes of the excitation functions but only lead to the shifting of the energy scale. With realistic isospin trend of  $V_b$   $\sigma_{cap}(^{40}\text{Ca}+^{124}\text{Sn}) < \sigma_{cap}(^{48}\text{Ca}+^{124}\text{Sn})$  and  $\sigma_{cap}(^{40}\text{Ca}+^{132}\text{Sn}) < \sigma_{cap}(^{48}\text{Ca}+^{132}\text{Sn})$  at energies above the corresponding Coulomb barriers.

## B. Effect of neutron transfer in reactions with beams $^{16,18}\text{O}$

Figures 4-7 show the capture excitation function for the reactions  $^{16,18}\text{O}+^{76,74}\text{Ge}$ ,  $^{16,18}\text{O}+^{94,92}\text{Mo}$ ,  $^{16,18}\text{O}+^{114,112,120,118,126,124}\text{Sn}$ , and  $^{16,18}\text{O}+^{52,50}\text{Cr}$  as a function of bombarding energy. One can see a rather good agreement between the calculated results and the experimental data [2, 13–15] for the reactions  $^{16}\text{O}+^{76}\text{Ge}$ ,  $^{16,18}\text{O}+^{92}\text{Mo}$ , and  $^{18}\text{O}+^{112,118,124}\text{Sn}$ . The  $Q_{2n}$ -values for the  $2n$ -transfer processes are positive (negative) for all reactions with  $^{18}\text{O}$  ( $^{16}\text{O}$ ). Thus, the neutron transfer can be important for the reactions with the  $^{16}\text{O}$  beam. However, our results show that cross sections for reactions  $^{16}\text{O}+^{76}\text{Ge}$  ( $^{16}\text{O}+^{114,120,126}\text{Sn}$ ,  $^{52}\text{Cr}$ ) and  $^{18}\text{O}+^{74}\text{Ge}$  ( $^{18}\text{O}+^{114,118,124}\text{Sn}$ ,  $^{50}\text{Cr}$ ) are very similar. The reason of such behavior is that after the  $2n$ -transfer in the system  $^{18}\text{O}+^{A-2}\text{X} \rightarrow ^{16}\text{O}+^A\text{X}$  the deformations remain to be similar. As a result, the corresponding Coulomb barriers of the systems  $^{18}\text{O}+^{A-2}\text{X}$  and  $^{16}\text{O}+^A\text{X}$  are almost the same and, correspondingly, their capture cross sections coincide. Just the same behavior was observed in the recent experiments  $^{16,18}\text{O}+^{76,74}\text{Ge}$  [2].

One can see in Figs. 4-7 that at energies above and near the Coulomb barrier the cross sections with and without two-neutron transfer are quite similar. After the  $2n$ -transfer (before the capture) in the reactions  $^{18}\text{O}(\beta_2 = 0.1) + ^{92}\text{Mo}(\beta_2 = 0.05) \rightarrow ^{16}\text{O}(\beta_2 = 0) + ^{94}\text{Mo}(\beta_2 = 0.151)$ ,  $^{18}\text{O}(\beta_2 = 0.1) + ^{74}\text{Ge}(\beta_2 = 0.283) \rightarrow ^{16}\text{O}(\beta_2 = 0) + ^{76}\text{Ge}(\beta_2 = 0.262)$ ,  $^{18}\text{O}(\beta_2 = 0.1) + ^{112}\text{Sn}(\beta_2 = 0.123) \rightarrow ^{16}\text{O}(\beta_2 = 0) + ^{114}\text{Sn}(\beta_2 = 0.121)$ ,  $^{18}\text{O}(\beta_2 = 0.1) + ^{118}\text{Sn}(\beta_2 = 0.111) \rightarrow ^{16}\text{O}(\beta_2 = 0) + ^{120}\text{Sn}(\beta_2 = 0.104)$ , and  $^{18}\text{O}(\beta_2 = 0.1) + ^{124}\text{Sn}(\beta_2 = 0.095) \rightarrow ^{16}\text{O}(\beta_2 = 0) + ^{126}\text{Sn}(\beta_2 = 0.09)$  the deformations of the nuclei decrease and the values of the corresponding Coulomb barriers increase. As a result, the transfer suppresses the capture process at the sub-barrier energies. The suppression becomes stronger with decreasing energy. As examples, in Fig. 4 and 5 we show this effect for the reactions  $^{18}\text{O}+^{74}\text{Ge}$ ,  $^{92}\text{Mo}$ .

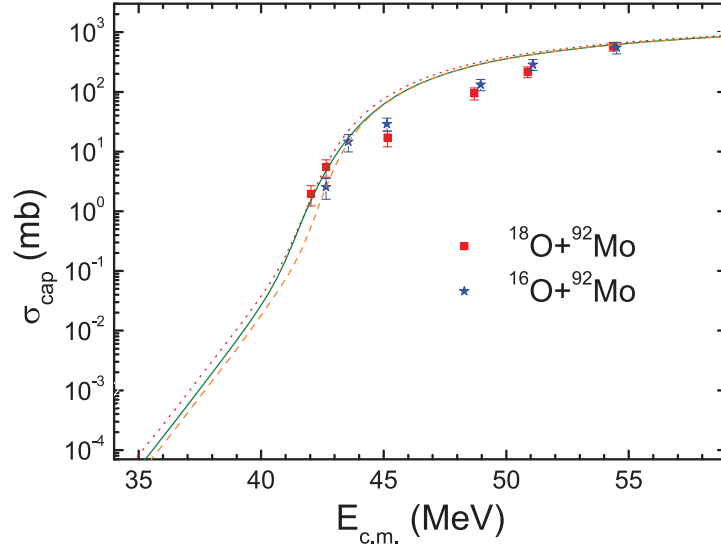


FIG. 5: (Colour online) The calculated capture cross sections versus  $E_{c.m.}$  for the reactions  $^{16}\text{O}+^{92}\text{Mo}$  (dashed line) and  $^{18}\text{O}+^{92}\text{Mo}$  (solid line). For the  $^{18}\text{O}+^{92}\text{Mo}$  reaction, the calculated capture cross sections without the neutron transfer are shown by dotted line. The experimental data for the reactions  $^{16}\text{O}+^{92}\text{Mo}$  (solid stars) and  $^{18}\text{O}+^{92}\text{Mo}$  (solid squares) are from Ref. [14].

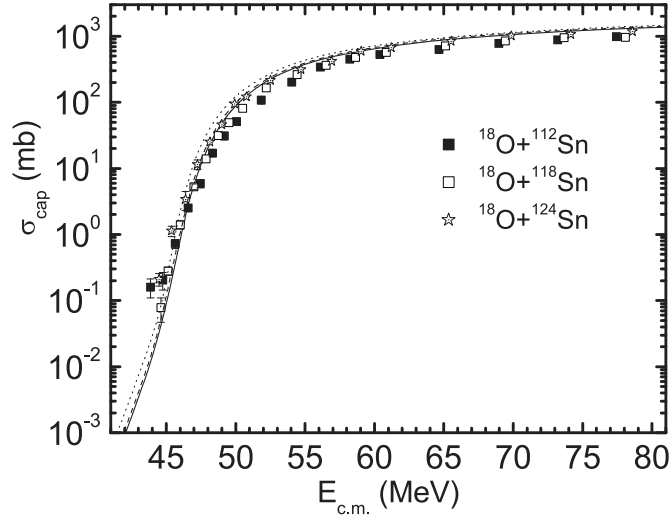


FIG. 6: The calculated capture cross sections versus  $E_{c.m.}$  for the reactions  $^{16}\text{O}+^{114}\text{Sn}$  and  $^{18}\text{O}+^{112}\text{Sn}$  (solid line),  $^{16}\text{O}+^{120}\text{Sn}$  and  $^{18}\text{O}+^{118}\text{Sn}$  (dashed line),  $^{16}\text{O}+^{126}\text{Sn}$  and  $^{18}\text{O}+^{124}\text{Sn}$  (dotted line). The calculated results for the reactions  $^{16}\text{O}+^{114,120,126}\text{Sn}$  and  $^{18}\text{O}+^{112,118,124}\text{Sn}$  coincide, respectively. The experimental data for the reactions  $^{18}\text{O}+^{112}\text{Sn}$  (solid squares),  $^{18}\text{O}+^{118}\text{Sn}$  (open squares), and  $^{18}\text{O}+^{124}\text{Sn}$  (open stars) are from Ref. [15].

### C. Capture and quasielastic barrier distributions

In Figs. 8 and 9, the calculated capture barrier distributions

$$D = d^2(E_{c.m.}\sigma_{cap})/dE_{c.m.}^2$$

for the reactions  $^{16}\text{O}+^{76}\text{Ge}$ ,  $^{144,154}\text{Sm}$  have only one pronounced maximum around  $E_{c.m.} = V_b$  as in the experiments [2, 16]. The calculated barrier distributions in Figs. 8 and 9 are slightly wider and fit the experimental data better than

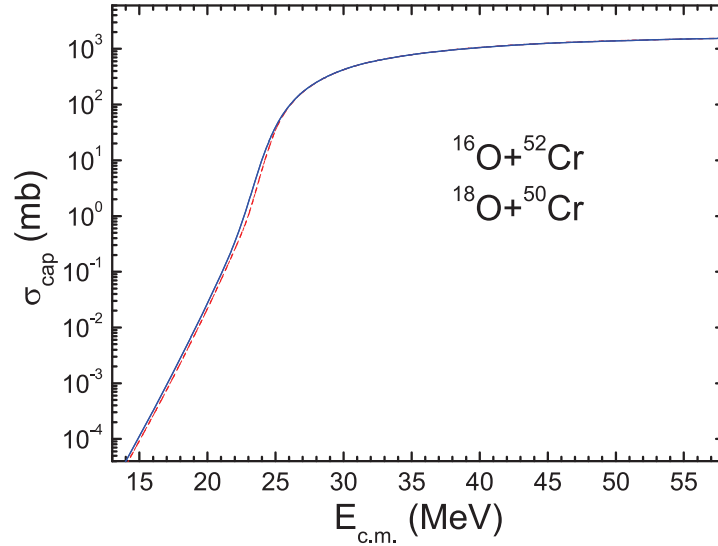


FIG. 7: (Colour online) The calculated capture cross sections versus  $E_{\text{c.m.}}$  for the reactions  $^{16}\text{O} + ^{52}\text{Cr}$  (dashed line) and  $^{18}\text{O} + ^{50}\text{Cr}$  (solid line).

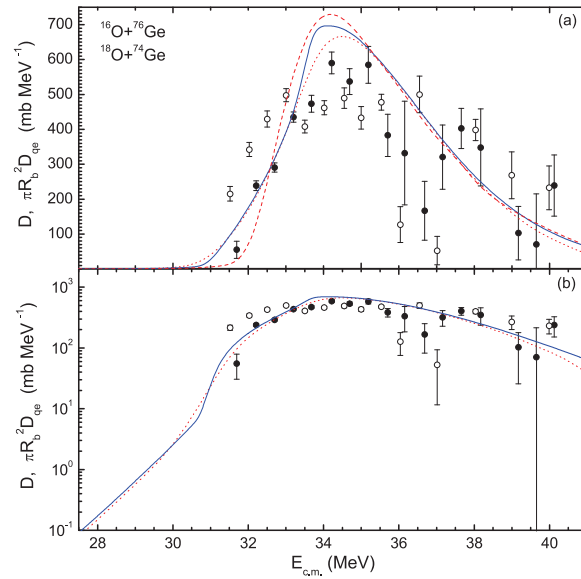


FIG. 8: (Colour online) (a) The calculated values of the quasielastic  $\pi R_b^2 D_{qe}$  (solid line) and capture  $D$  (dotted line) barrier distributions for the reactions  $^{16}\text{O} + ^{76}\text{Ge}$  and  $^{18}\text{O} + ^{74}\text{Ge}$ . The curves coincide for these reactions. The calculated  $D$  for the spherical interacting nuclei is shown by dashed line. The experimental data for the reactions  $^{16}\text{O} + ^{76}\text{Ge}$  (solid circles) and  $^{18}\text{O} + ^{74}\text{Ge}$  (open circles) are from Ref. [2]. (b) The calculated values of  $\pi R_b^2 D_{qe}$  (solid line) and  $D$  (dotted line) are shown in the logarithmic scale.

those obtained with the couple-channels approach in Fig. 5 of Ref. [2]. The capture (fusion) cross sections for the reactions  $^{16}\text{O} + ^{76}\text{Ge}$ ,  $^{144,154}\text{Sm}$  were well described with the quantum diffusion model in Ref. [5]. With almost spherical (deformed) target-nucleus we obtain a more narrow (wide) barrier distribution for the  $^{16}\text{O} + ^{144}\text{Sm}$  ( $^{16}\text{O} + ^{154}\text{Sm}$ ) reaction.

We compared the capture and the quasielastic barrier distributions for these reactions (Figs. 8 and 9). There is a direct relationship between the capture and the quasielastic scattering processes because any loss from the quasielastic

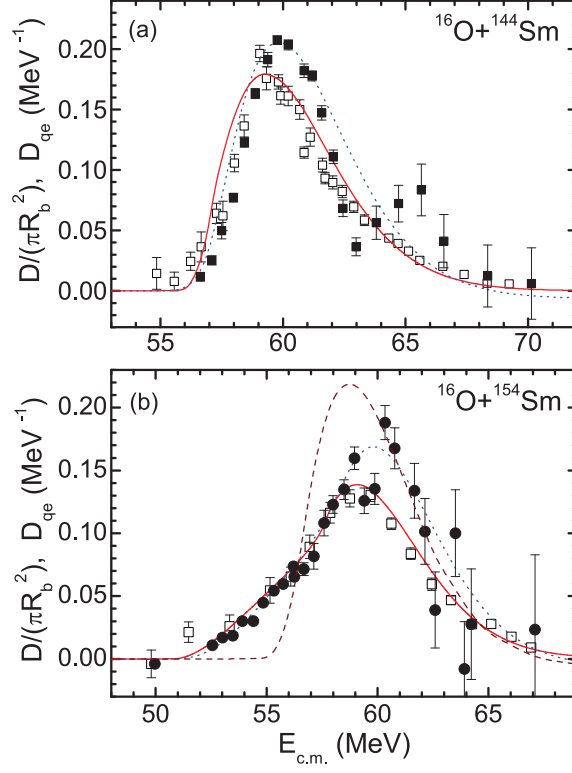


FIG. 9: (Colour online) The calculated values of quasielastic  $D_{qe}$  (solid line) and capture  $D/(\pi R_b^2)$  (dotted line) barrier distributions for the reactions  $^{16}\text{O} + ^{144}\text{Sm}$  (a) and  $^{16}\text{O} + ^{154}\text{Sm}$  (b). The experimental  $D_{qe}$  (open squares) and  $D/(\pi R_b^2)$  (solid circles) are from Ref. [16]. The calculated  $D$  for the spherical interacting nuclei is shown by dashed line (b).

channel contributes directly to the capture (the conservation of the reaction flux):

$$P_{qe}(E_{c.m.}, J) + P_{cap}(E_{c.m.}, J) = 1$$

and

$$dP_{cap}/dE_{c.m.} = -dP_{qe}/dE_{c.m.},$$

where  $P_{qe}$  is the reflection probability and  $P_{cap}$  is the capture (transmission) probability ( $J$  is the partial wave). The quasielastic barrier distribution is extracted by taking the first derivative of the  $P_{qe}(E_{c.m.}, J = 0)$  or  $P_{cap}(E_{c.m.}, J = 0)$  with respect to  $E_{c.m.}$ , that is,

$$D_{qe}(E_{c.m.}) = -dP_{qe}(E_{c.m.}, J = 0)/dE_{c.m.} = dP_{cap}(E_{c.m.}, J = 0)/dE_{c.m.}$$

So, by employing the quantum diffusion approach and calculating  $dP_{cap}(E_{c.m.}, J = 0)/dE_{c.m.}$ , one can obtain  $D_{qe}(E_{c.m.})$ . One can see in Figs. 8 and 9 that the shapes of the quasielastic and capture barrier distributions are similar. The same conclusion was experimentally obtained for the  $^{20}\text{Ne} + ^{208}\text{Pb}$  reaction in Ref. [17]. As in the case of capture barrier distribution, one can show that the width of the quasielastic barrier distribution increases with the deformation of the target-nucleus. In addition to the mean peak position of the  $D_{qe}$  around the barrier height, we observe the sharp change of the slope of  $D_{qe}$  or  $D$  below the Coulomb barrier energy because of a change of the regime of interaction (the external turning point leaves the region of the nuclear forces and friction [4, 5]) in the deep sub-barrier capture process (Fig. 8(b)).

#### IV. SUMMARY

As shown with the quantum diffusion approach, the capture cross sections for the reactions  $^{16}\text{O} + ^{52}\text{Cr}, ^{76}\text{Ge}, ^{94}\text{Mo}, ^{114}, ^{120}, ^{126}\text{Sn}$  and  $^{18}\text{O} + ^{50}\text{Cr}, ^{74}\text{Ge}, ^{92}\text{Mo}, ^{112}, ^{118}, ^{124}\text{Sn}$ , respectively, almost match. The fusion enhancement due to the positive  $Q_{2n}$ -value  $2n$ -transfer for  $^{18}\text{O} + ^{74}\text{Ge}$  has not been observed [2] because the

deformations of nuclei slightly decrease after the neutron transfer. This is different from the situation for the reactions  $^{40}\text{Ca}+^{124,132}\text{Sn}$  [3] with large positive  $Q_{2n}$ -values. The strong enhancements have been observed [3] in these reactions at sub-barrier energies because the deformation of light nucleus strongly increases (the heavy nucleus is spherical before and after transfer) after the two-neutron transfer.

We found that the shapes of the quasielastic and capture barrier distributions are similar. The sharp change of the slope of the quasielastic or capture barrier distribution is predicted at deep sub-barrier energy. This anomalous behavior of the barrier distribution is expected to be the experimental indication of a change of the regime of interaction in the sub-barrier capture. One concludes that the quasielastic technique could be an important tool in capture (fusion) research.

This work was supported by DFG, NSFC, and RFBR. The IN2P3(France) - JINR(Dubna) and Polish - JINR(Dubna) Cooperation Programmes are gratefully acknowledged. H.Q. Zhang is grateful to Chinese NSFC for the partial support.

- 
- [1] G. Montagnoli, *et al.*, Phys. Rev. C **85**, 024607 (2012); C. Simenel, Eur. Phys. J. A **48**, 152 (2012); C.A. Bertulani, EPJ Web Conf. **17**, 15001 (2011); Z. Kohley *et al.*, Phys. Rev. Lett. **107**, 202701 (2011); J.F. Liang, EPJ Web Conf. **17**, 02002 (2011); F. Scarlassara *et al.*, EPJ Web Conf. **17**, 05002 (2011).
  - [2] H.M. Jia *et al.*, Phys. Rev. C **86**, 044621 (2012).
  - [3] J.J. Kolata *et al.*, Phys. Rev. C **85**, 054603 (2012).
  - [4] V.V. Sargsyan, G.G. Adamian, N.V. Antonenko, and W. Scheid, Eur. Phys. J. A **45**, 125 (2010); Eur. Phys. J. A **47**, 38 (2011); Eur. Phys. J. A **48**, 118 (2012); Eur. Phys. J. A **49**, 19 (2013).
  - [5] V.V. Sargsyan, G.G. Adamian, N.V. Antonenko, W. Scheid, and H.Q. Zhang, Phys. Rev. C **84**, 064614 (2011); Phys. Rev. C **85**, 024616 (2012); Phys. Rev. C **86**, 014602 (2012).
  - [6] S. Ayik, B. Yilmaz, and D. Lacroix, Phys. Rev. C **81**, 034605 (2010).
  - [7] H. Hofmann, Phys. Rep. **284**, 137 (1997); S. Ayik, B. Yilmaz, A. Gokalp, O. Yilmaz, and N. Takigawa, Phys. Rev. C **71**, 054611 (2005); V.V. Sargsyan, Z. Kanokov, G.G. Adamian, and N.V. Antonenko, Part. Nucl. **41**, 175 (2010); G. Hupin and D. Lacroix, Phys. Rev. C **81**, 014609 (2010).
  - [8] R.A. Broglia, C.H. Dasso, S. Landowne, and A. Winther, Phys. Rev. C **27**, 2433 (1983); R.A. Broglia, C.H. Dasso, S. Landowne, and G. Pollarolo, Phys. Lett. B **133**, 34 (1983).
  - [9] S. Szilner *et al.*, Phys. Rev. C **76**, 024604 (2007); S. Szilner *et al.*, Phys. Rev. C **84**, 014325 (2011); L. Corradi *et al.*, Phys. Rev. C **84**, 034603 (2011).
  - [10] G.G. Adamian, A.K. Nasirov, N.V. Antonenko, and R.V. Jolos, Phys. Part. Nucl. **25**, 583 (1994); K. Washiyama, D. Lacroix, and S. Ayik, Phys. Rev. C **79**, 024609 (2009); S. Ayik, K. Washiyama, and D. Lacroix, Phys. Rev. C **79**, 054606 (2009).
  - [11] S. Raman, C.W. Nestor, Jr, and P. Tikkanen, At. Data Nucl. Data Tables **78**, 1 (2001).
  - [12] L.F. Canto, P.R.S. Gomes, J. Lubian, L.C. Chamon, and E. Crema, J. Phys. G **36**, 015109 (2009); Nucl. Phys. **A821**, 51 (2009).
  - [13] E.F. Aguilera, J.J. Kolata, and R.J. Tighe, Phys. Rev. C **52**, 3103 (1995).
  - [14] M. Benjelloun, W. Galster, and J. Vervier, Nucl. Phys. **A560**, 715 (1993).
  - [15] P. Jacobs, Z. Fraenkel, G. Mamane, and L. Tserruya, Phys. Lett. B **175**, 271 (1986).
  - [16] H. Timmers *et al.*, Nucl. Phys. **A584**, 190 (1995).
  - [17] E. Piasecki *et al.*, Phys. Rev. C **85**, 054608 (2012).